Article

Meteorological Drought Characterization in the Calabria Region (Southern Italy)

Roberto Coscarelli [1], Tommaso Caloiero [2,*], Eugenio Filice [3], Loredana Marsico [3] and Roberta Rotundo [3]

1   National Research Council-Research Institute for Geo-Hydrological Protection (CNR-IRPI), 87036 Rende, Italy; roberto.coscarelli@irpi.cnr.it
2   National Research Council-Institute for Agricultural and Forest Systems in Mediterranean (CNR-ISAFOM), 87036 Rende, Italy
3   Multi-Risk Functional Center, Regional Agency for Environmental Protection of Calabria, 88100 Catanzaro, Italy; e.filice@arpacal.it (E.F.); l.marsico@arpacal.it (L.M.); r.rotundo@arpacal.it (R.R.)
*   Correspondence: tommaso.caloiero@isafom.cnr.it or tommaso.caloiero@cnr.it; Tel.: +39-0984-841-464

Abstract: Due to the important role of water resources in the growth of the world's economy, drought causes global concern for its severe worldwide implications on different sectors, such as biodiversity, farming, public water supply, energy, tourism, human health, and ecosystem services. In particular, drought events can have strong environmental and socioeconomic impacts in countries depending on rain-fed agriculture such as the ones in the Mediterranean region, which, due to a detected increase in warming and precipitation decrease, is considered a climate change hotspot. In this context, in this paper, meteorological drought in the Calabria region (southern Italy) has been characterized considering the Standardized Precipitation Index (SPI) evaluated at different timescales. First, the temporal distribution of the most severe dry episodes has been evaluated. Then, a trend analysis has been conducted considering the different seasons, the wet (autumn and winter) and dry (spring and summer) periods, and the annual scale. Finally, the relationship between drought and some teleconnection patterns (the North Atlantic Oscillation—NAO, the El Niño–Southern Oscillation—ENSO, and the Mediterranean Oscillation—MO) has been investigated. Results show that the majority of the severe/extreme drought events have been observed between 1985 and 2008. Moreover, a decrease in SPI values has been observed in winter and spring, in both the wet and dry periods, and upon the annual scale considering the 12-month SPI and the 24-month SPI. Finally, a link between the drought episodes in the Calabria region and the NAO phases and the MO has been identified. Since drought episodes can severely impact water resources and their uses, the findings presented in this work can be useful to plan and manage the water supply for household, farming, and industrial uses.

Keywords: drought; SPI; trend; teleconnection patterns; Calabria

1. Introduction

Drought can be considered one of the major environmental disasters that can have a considerable impact on humanity. In fact, this phenomenon can lead to a deficiency in drinking water for both humans and livestock with a consequent reduction in agricultural production and an increase in economic costs [1,2]. Usually, four different types of droughts can be detected: meteorological, agricultural, hydrological, and socioeconomic drought [3,4]. The first three types of droughts are strictly related to a deficit in precipitation, soil moisture, and surface or groundwater, respectively [5,6]. Socioeconomic drought, on the other hand, characterizes the adverse conditions in a society, economy, and environment resulting from a reduced water supply [7,8].

Usually, drought monitoring depends on the analysis of a set of indicators representative of the different components of the hydrological cycle (e.g., precipitation, soil moisture, reservoir levels, river flow, groundwater levels) or specific impacts (vegetation stress), and starting from these indicators, many different indices have been developed over the

decades to measure drought. The evaluation of the indices can be considered the first step in drought management studies because they allow us to monitor drought conditions and to identify and characterize drought events [9]. In fact, generally, drought indices are evaluated as the statistical anomalies of the actual situation of an indicator with respect to the long-term average of this indicator at a given location and period of time, thus allowing these indices to express droughts in a region according to different drought categories. Nevertheless, no unique index is able to explain the several types of droughts (meteorological, agricultural, hydrological) and changes in the hydrometeorological regime [10]. As regards meteorological drought, several indices have been proposed in the literature in the past years, such as, for example, the Percent of Normal Index (PNI) [11], the Decimal Index (DI) [12], the Effective Drought Index (EDI) [13], the Standardized Precipitation Index (SPI) [14], and the Standardized Precipitation Evapotranspiration Index (SPEI) [15]. Among these indices of meteorological drought, the Standardized Precipitation Index (SPI) can be considered the most well-known and used [16]. This index measures the severity of anomalous dry events, which can be calculated for the accumulated precipitation during a given period (i.e., 1, 3, 6, 9, 12, 24 or 48 months) to estimate the different potential impacts of a meteorological drought. In fact, the SPI evaluated for short-term periods (from 1 to 3 months) is linked with immediate impacts such as reduced soil moisture, snowpack, and flow in smaller creeks that affect vegetation and agricultural practices. The SPI calculated for medium-term periods (from 3 to 12 months) is associated with reduced stream flow and reservoir storage. The SPI evaluated for long-term periods (from 12 to 48 months) is related to reduced reservoir and groundwater recharge with an implication for water resource management [17]. Nevertheless, the relationship between the accumulation period and drought impact is also influenced by the natural environment (e.g., geology, soils) and human intervention (e.g., existence of irrigation schemes). The Mediterranean Basin is characterized by water scarcity and recurrent drought, and for this reason, numerous studies have been performed to analyze drought in the Mediterranean Basin, especially using the SPI (e.g., [18]), and especially in Italy. In fact, for its location in the middle of the western Mediterranean and for its peculiar shape, extending over a wide latitude from north to south, Italy is particularly affected by drought events involving the Mediterranean area, especially from 1980 onward [19], and several studies on drought events have been carried out. As an example, a trend analysis of a 24-month SPI showed negative trends in large areas of the Mediterranean Basin [18]. Magno et al. [20] detected a tendency toward an increasing drought risk in several areas of the Mediterranean Basin such as central Spain and southern Italy. In Italy, Caloiero et al. [21] estimated the main drought characteristics (severity, duration, and intensity) by means of the run theory applied to SPI values, evidencing that several drought events with short duration and little severity could be expected.

Given this research context, the main objective of this study is to characterize meteorological drought in the Calabria region (southern Italy) by (i) identifying the major drought episodes affecting the region by means of the SPI, (ii) detecting the temporal tendencies of SPI values evaluated at different timescales, and (iii) investigating the possible relation between drought and some teleconnection indices. Even though this is not the first work aiming at characterizing meteorological drought in the Calabria region, it is the most updated work since past studies considered only observation periods ending in the early years of the 2000s. Moreover, while several papers have analyzed the relation between rainfall and teleconnection indices, the influence of these indices on SPI values in the Calabria region has not been properly investigated.

2. Materials and Methods

2.1. Study Area and Data

The Calabria region (15°37′—17°13′ E and 37°54′—40°09′ N) is located in the southernmost part of Italy and has a total area of 15,080 km^2 (Figure 1), with an altitude ranging from sea level to more than 2000 m [22].
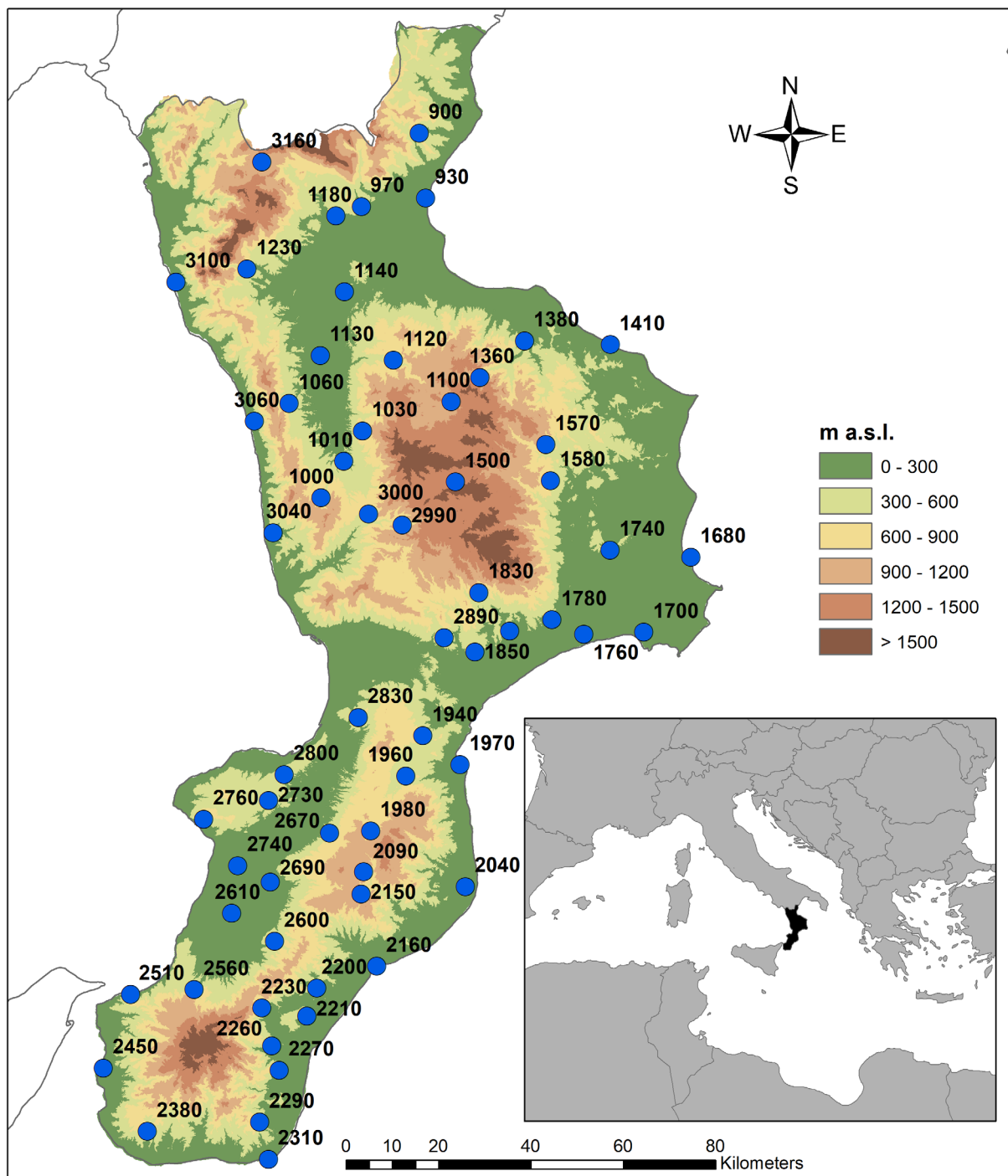
Figure 1. Study area and location of the selected rain gauges.

Following the Köppen–Geiger classification [23], the climate of the region is a hot-summer Mediterranean climate; therefore, one with hot summers and mild winters when the highest percentage of the mean annual rainfall occurs. As regards temperatures, the coldest month has an average temperature above 0 °C, while the average temperature reaches values higher than 20 °C. Moreover, local climate is influenced by the orography of the region, which constitutes a barrier between the warm air currents coming from Africa affecting the Ionian side and the western air currents affecting the Tyrrhenian side [24].

Since agriculture is one of the largest sectors of the tradable economy, a period of drought in Calabria can have significant ecological, social, and economic impacts. In fact, Calabria has experienced several rainfall deficits and drought events at the regional level,

and thus it has been adopted as the case study. Moreover, drought analysis presents several difficulties and challenges due to its complex nature and the diverse factors involved. One of the major challenges is data quality and availability at appropriate spatial and temporal scales that can hinder accurate drought analysis. In the present study, near-complete records of monthly rainfall data have been provided by the Multi-Risk Functional Centre of the Regional Agency for Environment Protection of the Calabria region for the period 1951–2022. The database consists of high quality rainfall data which have been extensively used in past climatological studies performed on the region (e.g., [24]). In particular, in order to perform a reliable statistical analysis, in this work, rainfall series with several missing records were discarded, and thus the analyses have been performed on 62 monthly rainfall series (Figure 1 and Table 1), with an average density of one station per 243 km^2.

2.2. Standardized Precipitation Index (SPI)

According to McKee et al. [14], given the precipitation amount recorded in a station, the SPI allows us to evaluate wet and dry spells and their characteristics (e.g., duration, severity, intensity). As stated by Hayes et al. [25], this index exhibits three primary advantages and three main disadvantages. The advantages of utilizing the SPI are as follows:

(i)   The simplicity of evaluating the SPI due to its reliance solely on rainfall data;

(ii)   The standardized nature of the SPI as an index, which ensures consistency in the frequency of extreme events across different locations and timescales;

(iii) The SPI allows for variable timescales, facilitating the analysis of drought dynamics.

However, there are also several disadvantages associated with the use of the SPI:

(i)   The assumption that an appropriate theoretical probability distribution can be identified to model the raw precipitation data, as different distributions can yield different outcomes;

(ii)   The length of the precipitation record significantly impacts SPI values. Varying record lengths may yield different results;

(iii) Misleadingly large positive or negative SPI values may arise when running the index at short timescales (1, 2, or 3 months) in regions with low seasonal precipitation.

For its advantages, the SPI is one of the most used and well-known indices and has been described in depth in several studies (see, e.g., [16]). The probability density function is evaluated as follows:

$$g(x) = \frac{1}{\beta^\alpha \Gamma(\alpha)} x^{\alpha-1} e^{-x/\beta} \text{ for } x > 0 \ \text{ and with } \Gamma(\alpha) = \int_0^\infty y^{\alpha-1} e^{-y} \mathrm{d}y \tag{1}$$

where x is the precipitation amount, and α and β are the shape and the scale parameter [26]. $\Gamma(\alpha)$ is the gamma function that is undefined for a null rainfall amount, and thus a modified cumulative distribution function (CDF) must be considered.

$$H(x) = q + (1-q)\, G(x), \tag{2}$$

where q is the probability of null precipitation, and $G(x)$ is the CDF:

$$G(x) = \int_0^x g(x)\mathrm{d}x = \frac{1}{\beta^\alpha \Gamma(\alpha)} \int_0^x x^{\alpha-1} e^{-x/\beta} \mathrm{d}x, \tag{3}$$

The SPI can be then evaluated as follows:

$$\mathrm{SPI} = \begin{cases} -\left(t - \frac{c_0 + c_1 t + c_2 t^2}{1 + d_1 t + d_2 t^2 + d_3 t^3}\right) 0 < \mathrm{H}(x) \leq 0.5 \ with \ t = \sqrt{\ln\left(\frac{1}{(H(x))^2}\right)} \\ +\left(t - \frac{c_0 + c_1 t + c_2 t^2}{1 + d_1 t + d_2 t^2 + d_3 t^3}\right) 0.5 < \mathrm{H}(x) \leq 1.0 \ with \ t = \sqrt{\ln\left(\frac{1}{(1-H(x))^2}\right)} \end{cases}, \tag{4}$$

with c_i and d_i coefficients. Table 2 shows the SPI classification proposed by McKee et al. [14].

Table 1. Selected rain gauges and percentages of missing data.

#ID	Name	Elevation	Percentage	#ID	Name	Elevation	Percentage
900	Albidona	810	85.4	2040	Monasterace–Punta Stilo	70	93.4
930	Villapiana Scalo	5	96.0	2090	Fabrizia	948	90.8
970	Cassano allo Ionio	251	98.6	2150	Fabrizia—Cassari	970	98.6
1000	Domanico	736	94.9	2160	Gioiosa Ionica	125	99.3
1010	Cosenza	242	97.0	2200	Antonimina	310	83.2
1030	San Pietro in Guarano	660	99.0	2210	Ardore Superiore	250	93.6
1060	Montalto Uffugo	468	86.5	2230	Plati'	300	96.9
1100	Cecita	1180	94.3	2260	San Luca	250	95.1
1120	Acri	790	95.1	2270	Sant'Agata del Bianco	380	97.3
1130	Torano Scalo	97	97.1	2290	Staiti	550	97.0
1140	Tarsia	203	87.3	2310	Capo Spartivento	48	96.0
1180	Castrovillari	353	96.3	2380	Montebello Ionico	470	96.8
1230	San Sosti	404	98.1	2450	Reggio Calabria	15	91.6
1360	Longobucco	770	95.8	2510	Scilla	73	98.5
1380	Cropalati	367	96.9	2560	Sinopoli	502	97.4
1410	Cariati Marina	10	97.7	2600	Cittanova	407	97.5
1500	Nocelle–Arvo	1315	96.5	2610	Rizziconi	114	94.3
1570	Savelli	964	83.2	2670	Arena	450	99.4
1580	Cerenzia	663	91.0	2690	Feroleto della Chiesa	160	95.5
1680	Crotone	5	96.2	2730	Mileto	368	95.0
1700	Isola di Capo Rizzuto–Campolongo	90	89.0	2740	Rosarno	61	96.1
1740	San Mauro Marchesato	288	73.5	2760	Joppolo	185	99.0
1760	Botricello	18	96.7	2800	Vibo Valentia	498	92.1
1780	Cropani	347	99.2	2830	Filadelfia	550	98.9
1820	Soveria Simeri	366	80.0	2890	Tiriolo	690	98.7
1830	Albi	710	95.2	2990	Parenti	830	90.1
1850	Catanzaro	334	99.2	3000	Rogliano	650	97.0
1940	Palermiti	480	98.4	3040	Amantea	54	93.7
1960	Chiaravalle Centrale	714	96.2	3060	Paola	160	97.3
1970	Soverato Marina	29	88.1	3100	Belvedere Marittimo	10	79.1
1980	Serra San Bruno	790	96.1	3160	Campotenese	965	98.2
900	Albidona	810	85.4	2040	Monasterace–Punta Stilo	70	93.4

Table 2. Climate classification according to SPI values.

SPI Value	Class	Probability (%)
SPI $\geq$ 2.00	Extremely wet	2.3
$1.50 \leq$ SPI < 2.00	Severely wet	4.4
$1.00 \leq$ SPI < 1.50	Moderately wet	9.2
$0.00 \leq$ SPI < 1.00	Mildly wet	34.1
$-1.00 \leq$ SPI < 0.00	Mild drought	34.1
$-1.50 \leq$ SPI < -1.00	Moderate drought	9.2
$-2.00 \leq$ SPI < -1.50	Severe drought	4.4
SPI < -2.00	Extreme drought	2.3

2.3. Trend Analysis

As regards the trend analysis, parametric and/or nonparametric tests can be applied. Parametric tests are based on assumptions about the distribution of the population from which the sample was taken. Nonparametric tests are not based on assumptions, that is, the data can be collected from a sample that does not follow a specific distribution. Following Totaro et al. [27], in this paper, the MK test has been applied. In fact, nonparametric tests are usually preferred to parametric ones because they are distribution-free and do not require knowledge of the parent distribution.

In order to detect the trend in SPI values, the widely known nonparametric test of Mann–Kendall (MK) [28,29] has been applied.

Given n data at times j and k ($j > k$), the statistic S is given by the following:

$$S = \sum_{k=1}^{n-1} \sum_{j=k+1}^{n} sgn\left(x_j - x_k\right), \tag{5}$$

in which the sign function can be equal to 1 (if $x_j > x_k$), 0 (if $x_j = x_k$), or -1 (if $x_j < x_k$).

Given the S values and the variance of S, the Mann–Kendall test statistic can be then evaluated as follows:

$$Z = \begin{cases} \frac{S-1}{\sqrt{Var(S)}} & for\ S > 0 \\ 0 & for\ S = 0, \\ \frac{S+1}{\sqrt{Var(S)}} & for\ S < 0 \end{cases} \tag{6}$$

2.4. Correlation between the SPI and NAO

With respect to the correlation analysis, the Pearson and Spearman correlation coefficients are the most widely used statistical measures when measuring the relationship between variables [30]. The fundamental difference between the two correlation coefficients is that the Pearson coefficient works with a linear relationship between the two variables, whereas the Spearman coefficient works with monotonic relationships as well, and for this reason, in this paper, the Pearson coefficient has been evaluated.

The connections between drought and large-scale atmospheric patterns has been investigated by means of the Pearson product-moment coefficient applied to the SPI NAO values provided by NOAA's National Centers for Environmental Information (NCEI). The statistical significance (95%) of the regression was checked by using the two-tailed test of the Student's t-distribution by evaluating the probability of rejecting the null hypothesis regarding the absence of any relationship for the values of t with (N-2) degrees of freedom.

3. Results

In this study, drought was expressed using the SPI on different timescales. Indeed, it is generally agreed that the SPI on short-term scales (e.g., 3 or 6 months) describes drought affecting vegetation and agricultural practices, while on long-term scales (e.g., 12 or 24 months), it is a broad proxy for water resource management [31].

Figure 2 shows the percentages of rain gauges with SPI values lower than -1.50 (severe/extreme drought) for each month of the observation period and for each temporal aggregation.

Generally, for all the temporal aggregations, dry events are more frequent and extensive from 1985 onward, when peaks of the percentages higher than 90% can be observed. Nevertheless, in more recent periods, these dry events show a lower frequency and temporal extension than before. In particular, as regards the 3-month SPI, more than 80% of the rain gauges show SPI values lower than -1.50 in 1985 and 2002. At the same time, percentages higher than 70% are identified in 1965, 1988, 1992, and 2001, while in 1954, 1984, 1997, and 2001, this percentage assumes values between 60% and 70%. The highest percentage of rain gauges with 6-month SPI values lower than -1.50 (about 95%) is identified in 2002, but in several months of the 1985–2008 period, percentages higher than 80% (1985 and 1992), 70% (1990, 1992, 2001 and 2002), and 60% (1990,1992, 1997 and 2000) are detected. The results obtained for the shortest timescales (i.e., 3 and 6 months) are strictly related with droughts affecting vegetation and agricultural practices and are confirmed by the ones obtained for the longest timescales (i.e., 12 and 24 months) that are a broad proxy for water resource management. In fact, for both the 12-month and 24-month SPIs, the 1985–2008 period is confirmed as the period with more frequent and extensive severe and extreme dry events. In particular, from January to April 2002 (in four consecutive months), more than 80% of the rain gauges show 12-month SPI values lower than -1.50, and this percentage reaches 90% in February and March. Diffuse drought events are also identified in 1989, 1990, and 1992 when severe/extreme drought values are detected in more than

70% of the rain gauges. Finally, 1962, 1989, 1990, 1992, and 2018 present a percentage of rain gauges with SPI values lower than −1.5 higher than 60%. The differences between the 1985–2008 period and the remaining observation period are marked for the 24-month SPI. In fact, only in the 1985–2008 period are relevant percentages of severe/extreme drought values observed, with values higher than 70% in 7 months of 1990.
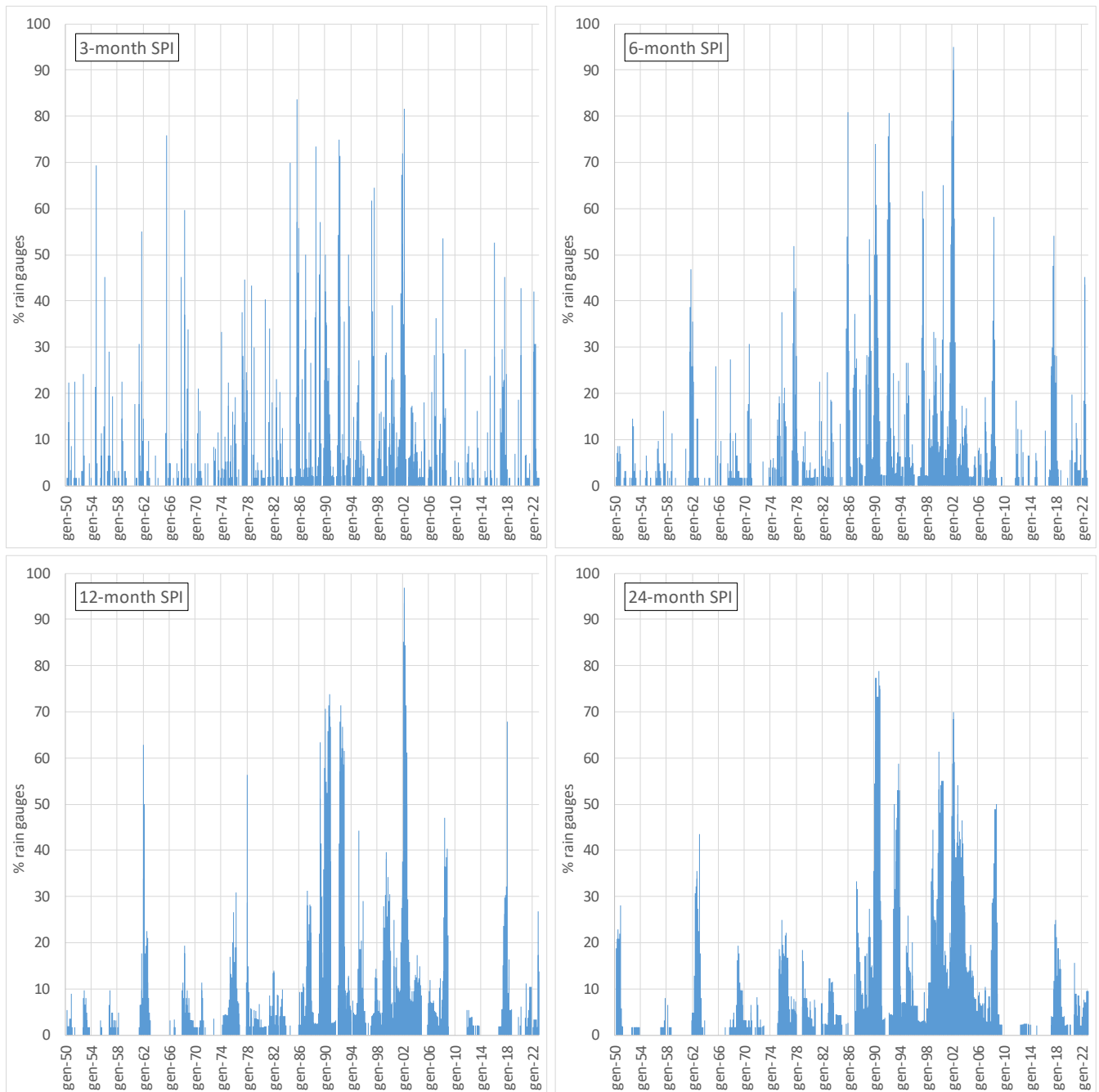

Figure 2. Time behavior of the percentage of rain gauges showing severe/extreme drought values.

Figure 3 shows a synthesis of the results of the application of the MK test on the SPI data evaluated for the various timescales and considering three different significance levels (SL = 90%, 95%, and 99%). In particular, the trend analysis was conducted considering the 3-month SPI for a seasonal analysis (SPI value in February for summer, May for autumn, August for winter, and November for spring), the 6-month SPI for the analysis of the wet and dry seasons (SPI value in February for the wet period and August for the dry period),

and the 12-month and 24-month SPIs for the annual analysis (December for both SPI-12 and SPI-24). Figure 4 shows the spatial distribution of the trend analysis for SL = 95%. As a result, a different trend emerges between winter and summer. In fact, a marked negative trend is detected in winter, with about 70% of rain gauges showing this behavior for SL = 90% and more than 50% for SL = 95%. On the contrary, in the summer season, even though the majority of the rain gauges (71%) did not show significant trends, only positive trends are identified (Figure 3). As regards the spatial distribution of the trends in the region (Figure 4), in winter, the negative values are not localized in any specific area, but they are well distributed over the whole region. Conversely, in summer, the positive trends are mainly present in some stations across the mountains in the central and southern part of Calabria. Moreover, some stations on the seaside of the southernmost areas of the region and on the northeastern side showed positive trends.

In spring, in more than 60% of the rain gauges, a not significant trend is detected (Figure 3). Nevertheless, the percentage of rain gauges with a negative trend (about 20% for SL = 95%) is higher than those with a positive one (about 3% for SL = 95%). These negative tendencies are mainly located in the southern areas of the region (Figure 4). As regards autumn, less than 10% of the rain gauges show significant trends for SL = 95%, negative in about 6% of the rain gauges and positive in about 3%, and almost all the rain gauges do not present any statistically significant trend (Figure 3). As a result, the spatial distribution of the trends do not show any particular behavior (Figure 4). The results obtained for the 3-month SPI obviously influence the tendencies of the wet and dry 6-month periods, evaluated with the application of the MK test to the 6-month SPI values.

In particular, the results obtained for the wet period are influenced by the results of winter, and thus the percentage of rain gauges presenting a negative trend (more than 40% for SL = 95%) is higher than those with a positive (about 3%) or not significant trend (Figure 3). Similar to the spatial distribution of the trend results obtained for the winter season, in the wet season, the negative values are distributed across the whole region (Figure 4). On the contrary, as regards the dry season (Figure 3), only a few rain gauges show significant trends, with negative values (more than 12% of the rain gauges for SL = 95%) prevailing over positive ones (about 5% of the rain gauges). From a spatial point of view, the negative values are mainly localized on the eastern side of the region (Figure 4). As regards the long-term periods, which are related with reduced reservoir and groundwater recharge with an implication for water resource management, the results obtained by means of the application of the MK test to the 12-month and 24-month SPIs show a marked prevalence of negative results over positive ones (Figure 3). In fact, in more than 30% and 40% of the rain gauges (SL = 95%), a negative tendency is identified for the 12-month and 24-month SPIs, respectively. This is mainly evident for the 24-month SPI, with a maximum percentage of stations with negative tendencies equal to 54.8% (SL = 90%). The spatial analysis of these results did not evidence a particular distribution of the trends, with the negative values distributed across all the region and the positive tendencies randomly localized in the region for both time aggregations (Figure 4).

Drought temporal evolution in the Mediterranean area and, specifically, in the study area can be correlated with changes in the intra-annual rainfall distribution, and thus it is usually linked with some teleconnection pattern.

Drought response to global circulation variability was first evaluated through a correlation analysis between drought and the NAO (Figure 5 and Table 3). Results evidenced a clear link between drought and the NAO values, in particular during winter and in the wet season. Specifically, in winter, 58.1% of the rain gauges are significantly correlated with the NAO values, especially in the western and central areas of the region. A similar result is obtained for the wet season, in which 50% of the rain gauges, mainly distributed in the western and central areas of the region, are well correlated with the NAO values. Relevant results are also obtained for the dry season, with about 30% of the rain gauges correlated with the NAO values. In the other time aggregations, the correlation is weaker than in the preceding ones, and the percentage of rain gauges correlated with the NAO is lower than 20%.
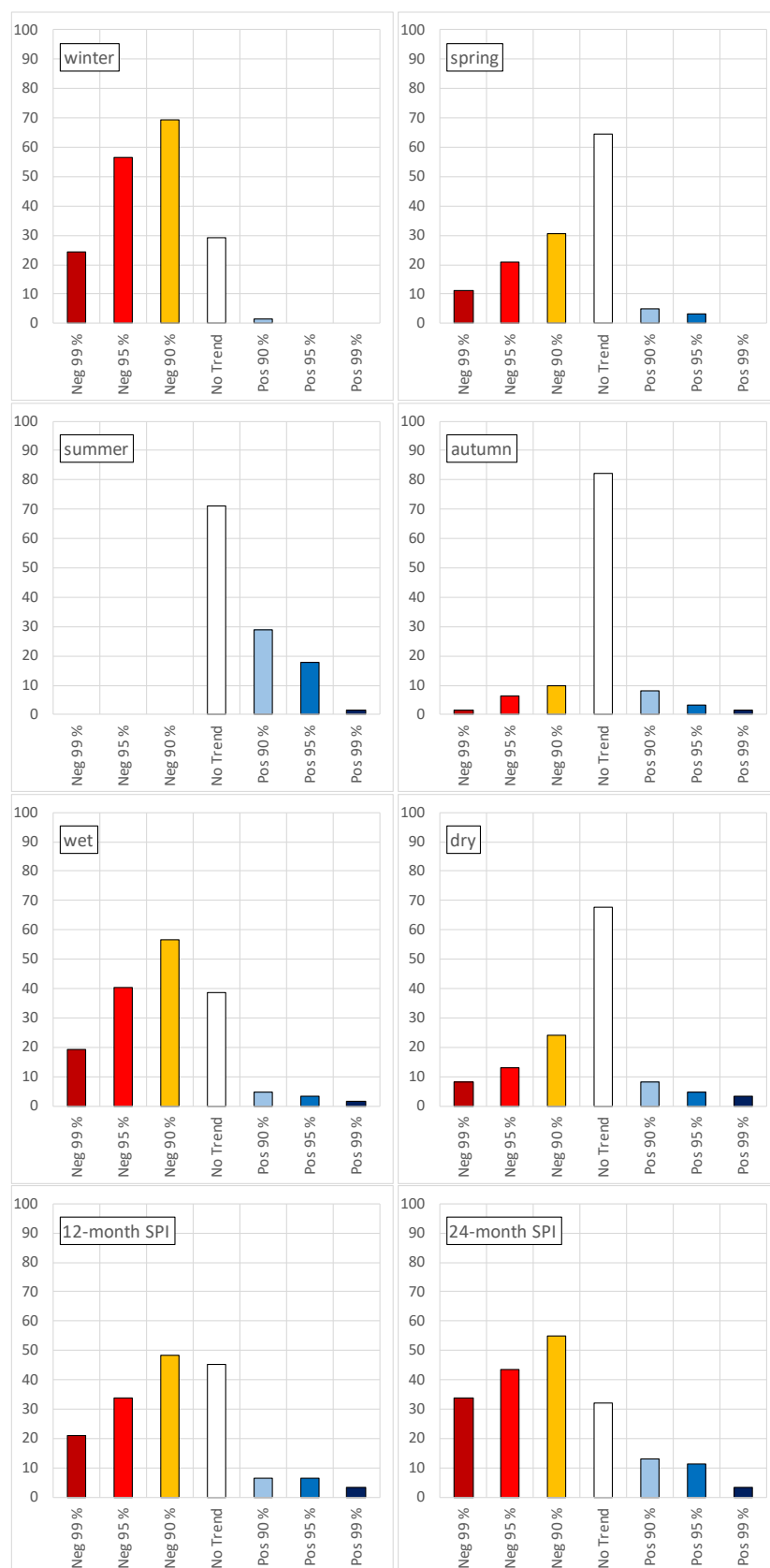
Figure 3. Results of the MK test expressed as a percentage of rain gauges showing negative or positive trends for three different significance levels (SL = 90%, 95%, and 99%).

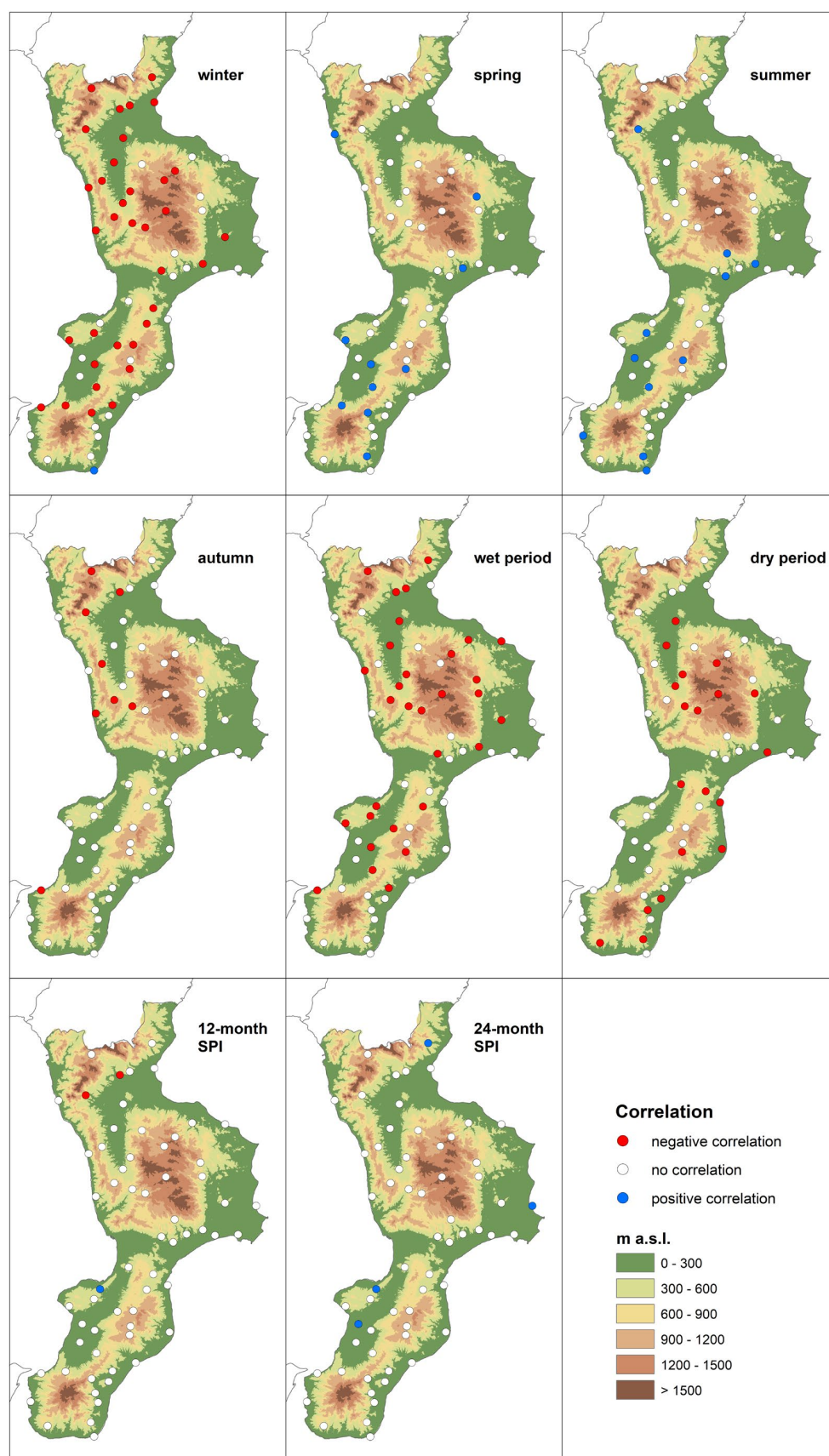**Figure 4.** Spatial results of the trend analysis (SL = 95%).

Figure 5. Correlation between the SPI and NAO values.

Table 3. Percentages of rain gauges correlated with the NAO values.

	Winter	Spring	Summer	Autumn	Dry Period	Wet Period	12-Month	24-Month
Negative Correlation	56.5	0.0	0.0	12.9	30.6	50.0	3.2	0.0
Positive Correlation	1.6	16.1	17.7	0.0	0.0	0.0	1.6	6.5
No Correlation	41.9	83.9	82.3	87.1	69.4	50.0	95.2	93.5

Drought response to global circulation variability was further analyzed considering a correlation analysis between drought and the ENSO (Figure 6 and Table 4). As a result, the ENSO did not show any particular correlation with SPI values. In fact, only in summer, about 30% of the rain gauges are significantly correlated with the ENSO values, especially on the southeastern side of the region. In the other time aggregations, the correlation is very weak, and the percentage of rain gauges correlated with the ENSO is lower than 5%, with the exception of the dry period (20.6%) and the 24-month timescale (11.1%).

Table 4. Percentages of rain gauges correlated with the ENSO values.

	Winter	Spring	Summer	Autumn	Dry Period	Wet Period	12-Month	24-Month
Negative Correlation	4.8	0.0	30.2	3.2	0.0	1.6	1.6	1.6
Positive Correlation	0.0	4.8	0.0	1.6	20.6	0.0	0.0	11.1
No Correlation	95.2	95.2	69.8	95.2	79.4	98.4	98.4	87.3

Finally, drought response to global circulation variability was evaluated through a correlation analysis between drought and the MO (Figure 7 and Table 5). Similar to the NAO, the results evidence a clear link between drought and the MO values, in particular during winter (73% of the rain gauges being significantly correlated) and in the wet season (57.1% of the rain gauges being significantly correlated). The percentage of rain gauges significantly correlated with the MO is thus higher than the one obtained with the NAO, involving almost all the region. Relevant results are also obtained in summer and for the 12-month SPI, with 27% and 36.5% of the rain gauges correlated with the MO values, respectively. In the other time aggregations, the correlation is weak, with values lower than 10%.

Table 5. Percentages of rain gauges correlated with the MO values.

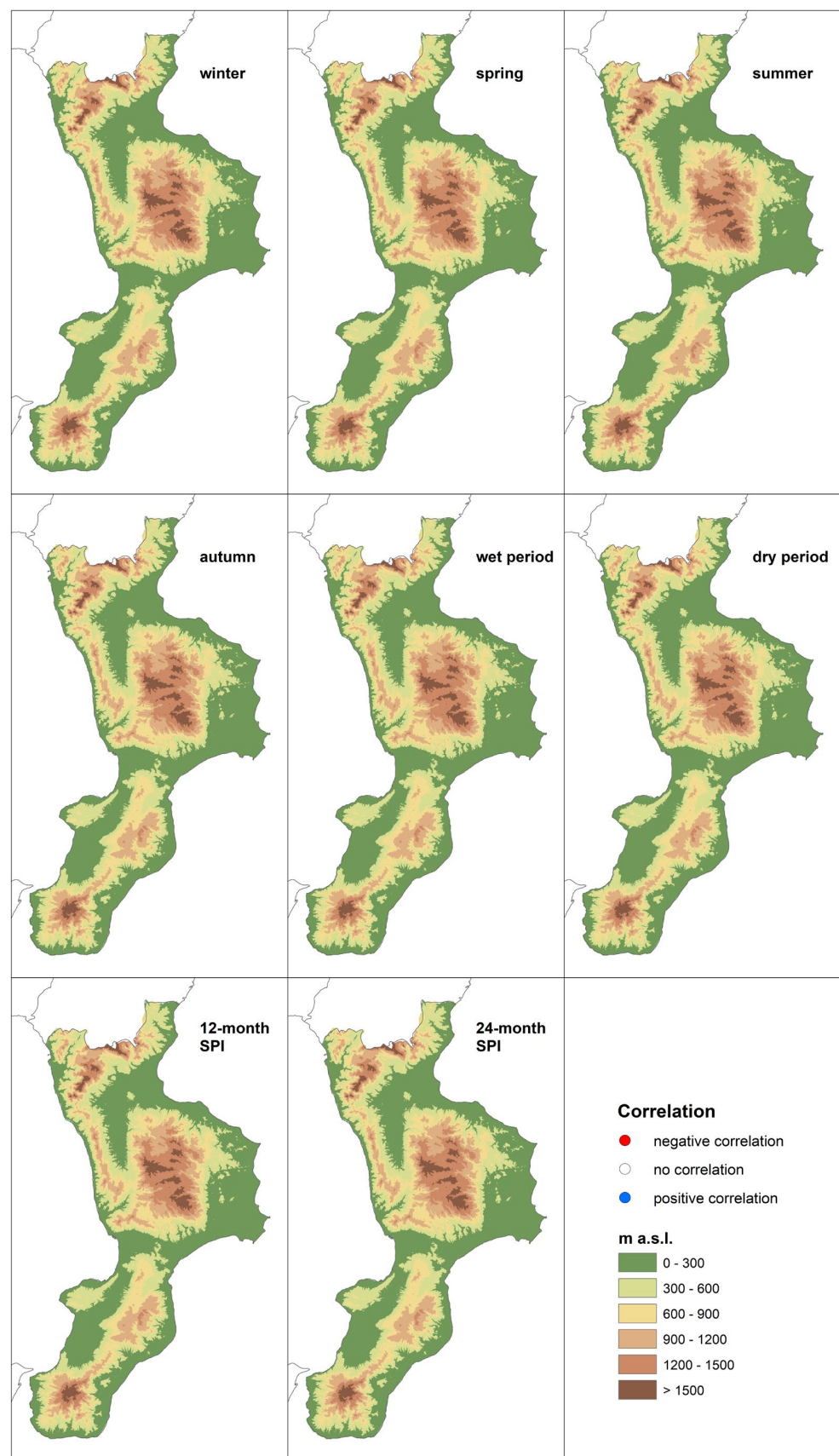|	Winter	Spring	Summer	Autumn	Dry Period	Wet Period	12-Month	24-Month
Negative Correlation	73.0	0.0	27.0	1.6	1.6	57.1	36.5	1.6
Positive Correlation	0.0	1.6	0.0	0.0	6.3	0.0	0.0	0.0
No Correlation	27.0	98.4	73.0	98.4	92.1	42.9	63.5	98.4

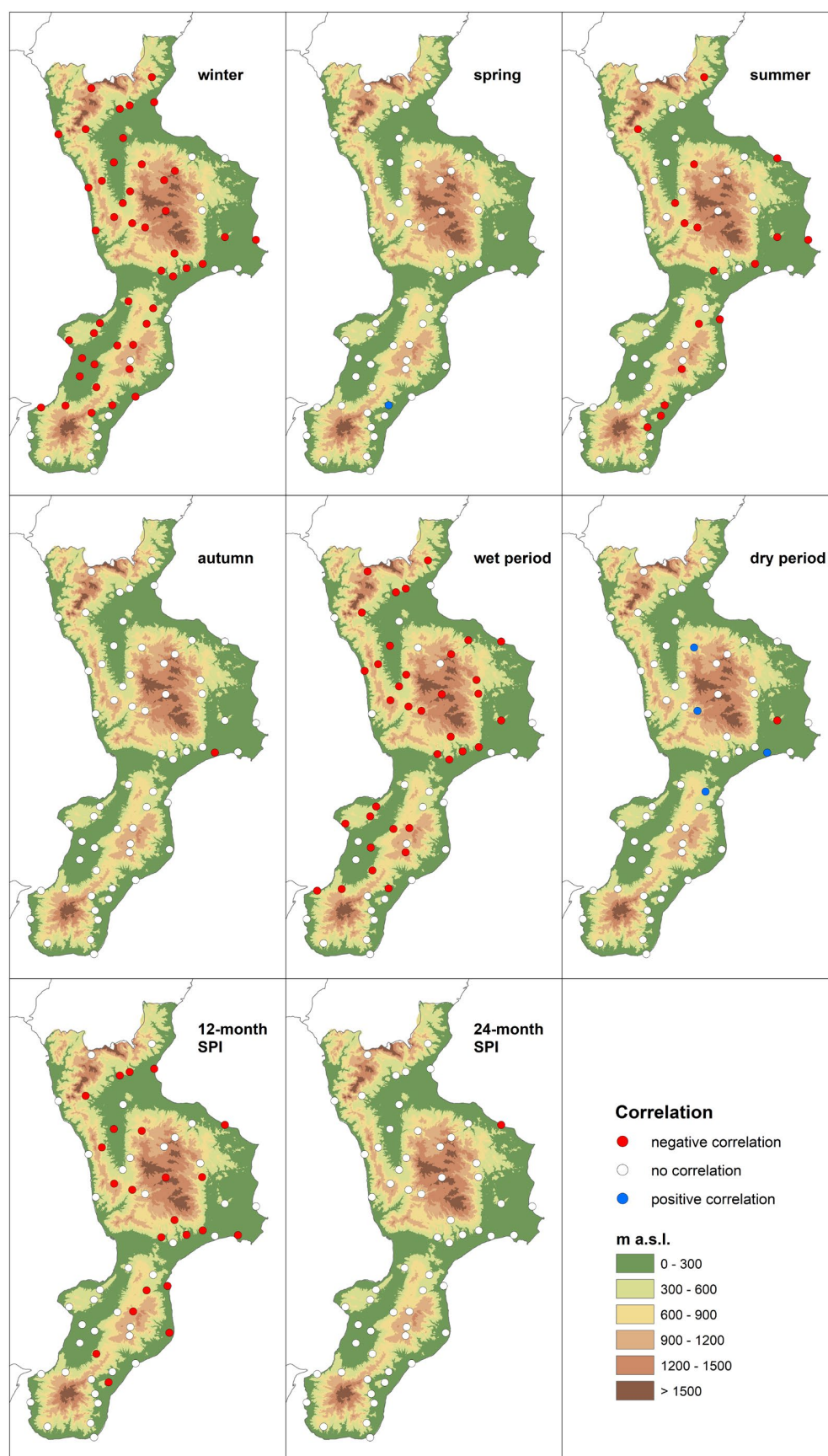**Figure 6.** Correlation between the SPI and ENSO values.

Figure 7. Correlation between the SPI and MO values.

4. Discussion

The agricultural sector plays a crucial role in the Calabria region's economy, providing employment opportunities and supporting rural communities. Although the Calabria region is a region with a lot of available water, with an annual average rainfall of more than 1000 mm, in recent years it has been grappling with the detrimental effects of drought which have significantly impacted the region's agricultural productivity, posing numerous challenges to farmers and the overall food security of the area. In fact, periods with insufficient rainfall and water availability have led to soil moisture deficits, hindered plant growth, and reduced crop yields. Crops such as cereals, vegetables, and fruits have suffered significant losses. Farmers have faced difficulties in cultivating their fields, resulting in reduced harvests and financial strains on agricultural livelihoods. Furthermore, drought has amplified the risk of wildfires in the Calabria region. In fact, parched vegetation and dry conditions create an ideal environment for the ignition and rapid spread of fires, leading to extensive damage to agricultural lands and natural habitats.

Continued research and innovation in drought analysis are essential to address the existing challenges and further advance our understanding of drought dynamics, improve monitoring and prediction capabilities, and enhance drought resilience and adaptation strategies. Within this context, in this paper, the major drought episodes affecting the region have been identified by means of the SPI, then the temporal tendencies of SPI values evaluated at different timescales have been evaluated and, finally, the possible relation between drought and some teleconnection indices has been investigated.

As regards the time behavior of the percentage of rain gauges showing severe/extreme drought values and the trend analysis, the results of this study are consistent with other studies on drought characterization performed in the Mediterranean area. In fact, the spatial and temporal extension of the drought events in the study area suggest that the majority of the severe/extreme drought events were observed between 1985 and 2008.

These results confirm the ones evidenced by Hoerling et al. [32] that detected an increase in drought episodes in the first decade of the 2000s and by Spinoni et al. [19], which identified that the highest drought frequency, duration, and severity were reached in the 1990s and 2000s. Moreover, the detected period includes the two widest and most devastating droughts of the last 40 years in the Mediterranean Basin (i.e., 1999–2001 and 2007–2012) [33]. The results of this study also confirm past trend studies performed on the same region (e.g., [34]); however, differently from these studies, in this paper, the observation period was extended until the end of 2022, and thus the results of the trend analysis are slightly different from the previous ones. In fact, while the overall trends are unchanged, different values of the percentage of stations where significant trends are detected have been observed. Nevertheless, the results of this study that evidenced a reduction in SPI values in the winter season, in the wet months, and on the annual scale and an increase in SPI values in the summer season confirm a tendency toward a reduction in the winter and annual rainfall and an increase in the summer rainfall identified in several Italian regions [35].

Finally, the results of this study confirm that drought temporal evolution in the Mediterranean area and, specifically, in the study area is usually correlated with changes in the intra-annual rainfall distribution, and thus it is linked with some teleconnection pattern [21]. In fact, drought in this region is mainly influenced by the NAO and, with a lower intensity, by other teleconnection patterns such as the ENSO [36]. In particular, in the study area, strong positive phases of the NAO tend to be associated with below-normal temperatures and below-normal precipitation, while opposite patterns of temperature and precipitation anomalies are typically observed during strong negative phases of the NAO [37]. These results evidencing a link between NAO phases and drought episodes in the Calabria region confirm past studies conducted in the Mediterranean region. In fact, several authors have acknowledged that the NAO is largely responsible for the periods of drought in this area (e.g., [38]). As an example, as evidenced by Kelley et al. [39], a marked negative phase of the NAO occurred between 1940 and 1980, and as a consequence,

this period is characterized by an above average rainfall in the Mediterranean Basin and positive SPI values. On the contrary, the dry conditions observed at the beginning of this century correspond to the positive SPI phase. As regards the ENSO, the low influence of this teleconnection pattern on the precipitation of the Calabria region has been identified in past studies [37], although it has been identified as one of the major drivers of drought events in other regions such as Turkey [40] or China [41].

In addition to the NAO and the ENSO, which represent the behavior of the atmosphere on a large scale, the results of this study evidenced a strong influence of the Mediterranean Oscillation (MO), thus confirming the results of Mathbout et al. [33] which detected its important role in severe, intense, and region-wide droughts, including the two most severe droughts in the region (1999–2001 and 2007–2012).

5. Conclusions

It is well known that drought events have significant negative effects on several aspects of the environment and society. The ongoing climate tendencies can determine an increase in the diffusion, intensity, and frequency of these events, mainly in areas, such as the Mediterranean Basin, considered hotspots for climate change. In this paper, an analysis of droughts in Calabria (southern Italy) has been carried out by means of the calculation of the SPI with an updated rainfall database. The application of the MK test clearly evidenced a negative significant tendency of SPI values in winter and globally in the wet 6-month period. These results deserve special attention if referred to Calabria for the impacts that the mentioned tendencies could have on water resource availability and agriculture. However, the diffuse negative correlation of the SPI with the NAO evaluated in the same seasons could determine a possibility to have forecast indications of future rainfall behaviors and thus enable the activation of adaptation measures for periods of particular drought. To conclude, it is important to add some final important remarks. The aim of this paper was to characterize meteorological drought in the Calabria region considering the SPI, thus evidencing some limitations in the study such as the spatial extension of the analysis and the detection of meteorological drought dependent on data availability. An improvement of this study could be the analysis of different types of droughts in a wider area considering, for example, remote sensing [42] that can provide valuable information, particularly for areas with limited ground-based observations. Moreover, future research could focus on different methodologies such as machine learning models [43,44].

Data Availability Statement: The data presented in this study are available on request from the corresponding authors.

Conflicts of Interest: The authors declare no conflict of interest.

References

1. Dracup, J.A.; Lee, K.S.; Paulson, E.G., Jr. On the definition of droughts. *Water Resour. Res.* **1980**, *16*, 297–302. [CrossRef]
2. Wilhite, D.A. Drought as a Natural Hazard: Concepts and Definitions. In *Drought: A Global Assessment*; Routledge: London, UK, 2000.
3. Van Loon, A.F. Hydrological drought explained. *WIREs Water* **2015**, *2*, 359–392. [CrossRef]
4. Wilhite, D.A.; Glantz, M.H. Understanding: The drought phenomenon: The role of definitions. *Water Int.* **1985**, *10*, 111–120. [CrossRef]
5. Mishra, A.K.; Singh, V.P. A review of drought concepts. *J. Hydrol.* **2010**, *391*, 202–216. [CrossRef]
6. Zhu, Y.; Wang, W.; Singh, V.P.; Liu, Y. Combined use of meteorological drought indices at multi-time scales for improving hydrological drought detection. *Sci. Total Environ.* **2016**, *571*, 1058–1068. [CrossRef] [PubMed]

7. Zhao, M.; Huang, S.; Huang, Q.; Wang, H.; Leng, G.; Xie, Y. Assessing socio-economic drought evolution characteristics and their possible meteorological driving force Assessing socio-economic drought evolution characteristics and their possible meteorological driving force. *Geomat. Nat. Hazards Risk* **2019**, *10*, 1084–1101. [CrossRef]

8. Zseleczky, L.; Yosef, S. Are Shocks Really Increasing? A Selective Review of the Global Frequency, Severity, Scope, and Impact of Five Types of Shocks. In Proceedings of the 2020 Conference Papers 5; International Food Policy Research Institute (IFPRI): Washington, DC, USA, 2014.

9. Wilhite, D.A. *Drought and Water Crises: Science, Technology, and Management Issues*; CRC Press: Boca Raton, FL, USA, 2014.

10. Wilhite, D.; Pulwarty, R.S. *Drought and Water Crises: Integrating Science, Management, and Policy*; CRC Press: Boca Raton, FL, USA, 2017.

11. World Meteorological Organization (WMO); Global Water Partnership (GWP). *Handbook of Drought Indicators and Indices*; Svoboda, M., Fuchs, B.A., Eds.; Integrated Drought Management Programme (IDMP): Geneva, Switzerland, 2016.

12. Gibbs, W.J.; Maher, J.V. *Rainfall Deciles as Drought Indicators*; Bureau of Meteorology Bulletin No. 48; Bureau of Meteorology: Melbourne, Australia, 1967.

13. Byun, H.R.; Wilhite, D.A. Objective Quantification of Drought Severity and Duration. *J. Clim.* **1999**, *12*, 2747–2756. [CrossRef]

14. McKee, T.B.; Doesken, N.J.; Kleist, J. The Relationship of Drought Frequency and Duration to Time Scales. In Proceedings of the Eighth Conference on Applied Climatology, Anaheim, CA, USA, 17–22 January 1993; pp. 179–184.

15. Vicente-Serrano, S.M.; Beguería, S.; López-Moreno, J.I. A multiscalar drought index sensitive to global warming: The standardized precipitation evapotranspiration index. *J. Clim.* **2010**, *23*, 1696–1718. [CrossRef]

16. Achite, M.; Simsek, O.; Adarsh, S.; Hartani, T.; Caloiero, T. Assessment and monitoring of meteorological and hydrological drought in semiarid regions: The Wadi Ouahrane basin case study (Algeria). *Phys. Chem. Earth* **2023**, *130*, 103386. [CrossRef]

17. Balacco, G.; Alfio, M.R.; Fidelibus, M.D. Groundwater Drought Analysis under Data Scarcity: The Case of the Salento Aquifer (Italy). *Sustainability* **2022**, *14*, 707. [CrossRef]

18. Caloiero, T.; Veltri, S.; Caloiero, P.; Frustaci, F. Drought Analysis in Europe and in the Mediterranean Basin Using the Standardized Precipitation Index. *Water* **2018**, *10*, 1043. [CrossRef]

19. Spinoni, J.; Naumann, G.; Vogt, J.V.; Barbosa, P. The biggest drought events in Europe from 1950 to 2012. *J. Hydrol. Reg. Stud.* **2015**, *3*, 509–524. [CrossRef]

20. Magno, R.; Pasqui, M.; Di Giuseppe, E. Analysis of changes in drought occurrence over the Mediterranean Basin using multiple time scales SPI index. In Proceedings of the 16th EMS Annual Meeting & 11th European Conference on Applied Climatology (ECAC), Trieste, Italy, 12–16 September 2016.

21. Caloiero, T.; Caroletti, G.N.; Coscarelli, R. IMERG-Based Meteorological Drought Analysis over Italy. *Climate* **2021**, *9*, 65. [CrossRef]

22. Buttafuoco, G.; Caloiero, T. Drought events at different timescales in southern Italy (Calabria). *J. Maps* **2014**, *10*, 529–537. [CrossRef]

23. Köppen, W. *Das Geographische System der Klimate*; Handbuch der, Klimatologie; Köppen, W., Geiger, R., Eds.; Verlag von Gebrüder Borntraeger: Berlin, Germany, 1936; Volume 1, pp. 1–44.

24. Buttafuoco, G.; Caloiero, T.; Ricca, N.; Guagliardi, I. Assessment of drought and its uncertainty in a southern Italy area (Calabria region). *Measurement* **2018**, *113*, 205–210. [CrossRef]

25. Hayes, M.J.; Svoboda, M.D.; Wilhite, D.A.; Vanyarkho, O.V. Monitoring the 1996 drought using the standardized precipitation index. *Bull. Am. Meteorol. Soc.* **1999**, *80*, 429–438. [CrossRef]

26. Thom, H.C.S. A note on the gamma distribution. *Mon. Weather Rev.* **1958**, *86*, 117–122. [CrossRef]

27. Totaro, V.; Gioia, A.; Iacobellis, V. Numerical investigation on the power of parametric and nonparametric tests for trend detection in annual maximum series. *Hydrol. Earth Syst. Sci.* **2020**, *24*, 473–488. [CrossRef]

28. Mann, H.B. Nonparametric Tests Against Trend. *Econometrica* **1945**, *13*, 245–259. [CrossRef]

29. Kendall, M.G.; Stuart, A. *The Advanced Theory of Statistics*; Macmillan: New York, NY, USA, 1977.

30. Caroletti, G.N.; Coscarelli, R.; Caloiero, T. A sub-regional approach to the influence analysis of teleconnection patterns on precipitation in Calabria (Southern Italy). *Int. J. Clim.* **2021**, *41*, 4574–4586. [CrossRef]

31. Caloiero, T. Drought analysis in New Zealand using the standardized precipitation index. *Environ. Earth Sci.* **2017**, *76*, 569. [CrossRef]

32. Hoerling, M.; Eischeid, J.; Perlwitz, J.; Quan, X.; Zhang, T.; Pegion, P. On the increased frequency of Mediterranean drought. *J. Clim.* **2012**, *25*, 2146–2161. [CrossRef]

33. Mathbout, S.; Lopez-Bustins, J.A.; Royé, D.; Martin-Vide, J. Mediterranean-Scale Drought: Regional Datasets for Exceptional Meteorological Drought Events during 1975–2019. *Atmosphere* **2021**, *12*, 941. [CrossRef]

34. Buttafuoco, G.; Caloiero, T.; Coscarelli, R. Analyses of drought events in Calabria (Southern Italy) using standardized precipitation index. *Water Resour. Manag.* **2015**, *29*, 557–573. [CrossRef]

35. Caloiero, T.; Veltri, S. Drought Assessment in the Sardinia Region (Italy) During 1922–2011 Using the Standardized Precipitation Index. *Pure Appl. Geophys.* **2019**, *176*, 925–935. [CrossRef]

36. Lloyd-Huhes, B.; Saunders, M.A. A drought climatology for Europe. *Int. J. Climatol.* **2002**, *22*, 1571–1592. [CrossRef]

37. Caloiero, T.; Coscarelli, R.; Ferrari, E.; Mancini, M. Precipitation change in Southern Italy linked to global scale oscillation indexes. *Nat. Hazards Earth Syst. Sci.* **2011**, *11*, 1683–1694. [CrossRef]

38. Vicente-Serrano, S.M.; López-Moreno, J.I.; Lorenzo-Lacruz, J.; El Kenawy, A.; Azorin-Molina, C.; Morán-Tejeda, E.; Pasho, E.; Zabalza, J.; Begueria, S.; Angulo-Martinez, M. The NAO impact on droughts in the Mediterranean region. In *HydroLogical, Socioeconomic and Ecological Impacts of the North Atlantic Oscillation in the Mediterranean Region Advances in Global Change Research*; Springer: Dordrecht, The Netherlands, 2011.

39. Kelley, C.; Ting, M.; Seager, R.; Kushnir, Y. Mediterranean precipitation climatology, seasonal cycle, and trend as simulated by CMIP5. *Geophys. Res. Lett.* **2012**, *39*, L21703. [CrossRef]

40. Abdelkader, M.; Yerdelen, C. Hydrological Drought Variability and Its Teleconnections with Climate Indices. *J. Hydrol.* **2022**, *605*, 127290. [CrossRef]

41. Yang, R.; Xing, B. Teleconnections of Large-Scale Climate Patterns to Regional Drought in Mid-Latitudes: A Case Study in Xinjiang, China. *Atmosphere* **2022**, *13*, 230. [CrossRef]

42. Zhao, C.; Huang, Y.; Li, Z.; Chen, M. Drought monitoring of Southwestern China using insufficient GRACE data for the long-term mean reference frame under global change. *J. Clim.* **2018**, *31*, 6897–6911. [CrossRef]

43. Sattari, M.T.; Falsafian, K.; Irvem, A.; Qasem, S.N. Potential of kernel and tree-based machine-learning models for estimating missing data of rainfall. *Eng. Appl. Comput. Fluid Mech.* **2020**, *14*, 1078–1094. [CrossRef]

44. Wang, G.C.; Zhang, Q.; Band, S.S.; Dehghani, M.; Chau, K.W.; Tho, Q.T.; Zhu, S.; Samadianfard, S.; Mosavi, A. Monthly and Seasonal Hydrological Drought Forecasting Using Multiple Extreme Learning Machine Models. *Eng. Appl. Comput. Fluid Mech.* **2022**, *16*, 1364–1381. [CrossRef]